Michael Januszyk,[1,2] Michael Sorkin,[1] Jason P. Glotzbach,[1] Ivan N. Vial,[1] Zeshaan N. Maan,[1] Robert C. Rennert,[1] Dominik Duscher,[1] Hariharan Thangarajah,[1] Michael T. Longaker,[1] Atul J. Butte,[3] and Geoffrey C. Gurtner[1]

# Diabetes Irreversibly Depletes Bone Marrow–Derived Mesenchymal Progenitor Cell Subpopulations

*Diabetes 2014;63:3047–3056 | DOI: 10.2337/db13-1366*

**Diabetic vascular pathology is largely attributable to impairments in tissue recovery from hypoxia. Circulating progenitor cells have been postulated to play a role in ischemic recovery, and deficiencies in these cells have been well described in diabetic patients. Here, we examine bone marrow–derived mesenchymal progenitor cells (BM-MPCs) that have previously been shown to be important for new blood vessel formation and demonstrate significant deficits in the context of diabetes. Further, we determine that this dysfunction is attributable to intrinsic defects in diabetic BM-MPCs that are not correctable by restoring glucose homeostasis. We identify two transcriptionally distinct subpopulations that are selectively depleted by both type 1 and type 2 diabetes, and these subpopulations have provasculogenic expression profiles, suggesting that they are vascular progenitor cells. These results suggest that the clinically observed deficits in progenitor cells may be attributable to selective and irreversible depletion of progenitor cell subsets in patients with diabetes.**

Diabetes has become an epidemic in the industrialized world (1). In the U.S., the annual incidence of diabetes has tripled since 1980 (2). Given this trend, it has been estimated that the total prevalence of diabetes in the U.S. will more than double by 2050, an occurrence that will place an enormous burden on the nation's health care system (3). While diabetes affects many aspects of human physiology, cardiovascular complications are the most common cause of morbidity and mortality in diabetic patients (4–6). Specifically, diabetes causes dysfunction of the mature endothelium and impaired neovascularization in response to ischemia, as evidenced by the reduced growth of collateral coronary vessels after acute myocardial infarction and the poor clinical outcomes associated with diabetic peripheral arterial disease (7–9).

In the absence of diabetes, we and others have shown that neovascularization in response to ischemic injury progresses partially through the recruitment of bone marrow–derived progenitor cells into ischemic tissues via the circulation, a process termed vasculogenesis (10–13). This recruitment is dependent upon successful stabilization of the transcription factor hypoxia-inducible factor (HIF)-1α in response to local hypoxia. HIF-1α drives the expression of numerous genes (14,15), including the chemokine CXCL12 (SDF-1), which functions as an endocrine and paracrine signal for progenitor cell recruitment into ischemic tissue (16), and vascular endothelial growth factor (VEGF), which promotes endothelial differentiation and proliferation of recruited progenitor cells (17,18). Conversely, in the setting of diabetes we have described deficits in HIF function both in local ischemic tissue (19) and in specific remote cell populations, including fibroblasts (20), adipose-derived stromal cells (21), and circulating endothelial progenitor cells (EPCs) (22,23).

[1]Division of Plastic and Reconstructive Surgery, Department of Surgery, Stanford University School of Medicine, Stanford, CA
[2]Program in Biomedical Informatics, Stanford University School of Medicine, Stanford, CA
[3]Division of Systems Medicine, Department of Pediatrics, Stanford University School of Medicine, Stanford, CA
Corresponding author: Geoffrey C. Gurtner, ggurtner@stanford.edu.

Received 5 September 2013 and accepted 10 April 2014.
This article contains Supplementary Data online at http://diabetes.diabetesjournals.org/lookup/suppl/doi:10.2337/db13-1366/-/DC1.

M.J. and M.S. contributed equally to this work.

EPCs are of particular interest, as their precise origin and their function in ischemic injury remain obscure. Hematopoietic stem cells (HSCs) and mesenchymal progenitor cells (MPCs) are generally regarded as the two most likely sources (24–26), although at present most evidence refutes the notion that HSCs are able to adopt nonhematopoietic fates (27–30). The case for a mesenchymal origin of EPCs rests on their ability to differentiate into endothelial cells and vascular smooth muscle in vitro (31–33). In addition, it has been shown that bone marrow–derived MPCs (BM-MPCs) contribute to postnatal vasculogenesis (17,34–36), and some groups have suggested a supportive role for these cells as vascular pericytes that promote vasculogenesis locally through the release of growth factors (37,38). Recently, we identified a candidate bone marrow–derived murine MPC population in vivo that is lineage negative, CD45 negative, and Sca-1 positive that responds to peripheral tissue ischemia by increasing in number in the peripheral circulation (17). Other groups have demonstrated that these cells express multiple embryonic stem cell genes, are mobilized into the circulation by GM-CSF, and differentiate into multiple tissue lineages under coculture conditions (39). Despite such advances in the characterization and function of BM-MPCs, little work has been done to define the effect of diabetes on these cells.

In this study, we examine BM-MPCs that have previously been shown to be important for new blood vessel formation (17,39) and demonstrate significant deficits in the context of diabetes. Further, we determine that this dysfunction is attributable to intrinsic defects in diabetic BM-MPCs that are not correctable by restoring glucose homeostasis. Since MPCs are a heterogeneous group of cells (40), we also examined gene expression at single cell resolution. Using this approach, we identified two transcriptionally distinct subpopulations that are selectively depleted by both type 1 and type 2 diabetes. These depleted subpopulations have a proangiogenic and vasculogenic gene expression profile suggesting that they are vascular progenitor cells. These results suggest that the clinically observed deficits in human progenitor cells may be attributable to selective and irreversible depletion of progenitor cell subsets in patients with diabetes.

## RESEARCH DESIGN AND METHODS

### Animals

Wild-type (WT) mice (C57BL/6) and *db/db* mice (BKS.Cg-$m^{+/+}$ Lepr$^{db}$) were purchased from The Jackson Laboratory (Bar Harbor, ME). Type 1 diabetes was induced in the former group with five consecutive daily injections of 50 mg/kg streptozotocin (STZ) (Sigma-Aldrich, St. Louis, MO) in sodium citrate (41). Two and 4 weeks after the last injection, blood glucose levels were assessed using a glucometer (Roche Bioproducts, Basel, Switzerland). Mice with capillary blood glucose levels <400 g/dL were excluded. Animal care was provided in accordance with the Stanford University School of Medicine guidelines and policies for the use of laboratory animals. All protocols were approved by the Administrative Panel on Laboratory Animal Care at the Stanford University School of Medicine.

### BM-MPC Harvest, Culture, and In Vitro STZ Exposure

After euthanasia, mice femora and tibiae were harvested and washed in serial dilutions of Betadine (Purdue Frederick Co., Norwalk, CT). Epiphyseal plates were removed and bones were flushed with 2% FBS in PBS to retrieve the marrow plugs. Plugs were then dissociated by trituration, filtered through a 100-μm cell strainer, and pelleted by centrifugation at 300*g* for 10 min. Cells were then resuspended in DMEM with 10% FBS and 1% penicillin/streptomycin (Life Technologies, Grand Island, NY) in 1 g/L glucose for normoglycemia and at 4.5 g/L glucose for hyperglycemia. Total bone marrow was then plated at $1 \times 10^6$ cells/cm$^2$ on tissue culture plastic. Cells were subcultured at 80–90% confluence and used after passage three. Hyperglycemic memory was investigated by placing diabetic cells in normoglycemic medium after passage one. The direct cellular effects of STZ were assessed by exposing WT BM-MPCs to medium with a 1.8 mmol/L STZ concentration for 30 min at 37°C, after which the medium was changed and the cells were passaged once before being assayed (42). Single cell gene expression analysis was performed on primary cells isolated from marrow plugs.

### In Vitro Hypoxia

In vitro hypoxia experiments were performed with a customized hypoxic incubator (Biospherix X Vivo Hypoxia Chamber). Experiments were performed at oxygen concentrations of 21% (hyperoxia) and 1% (hypoxia).

### HIF-1 Reporter Assay

Murine HIF-1 luciferase reporter constructs (p5xHRE) were previously created by cloning five tandem repeats of the VEGF hypoxia responsive element (HRE) into the pGL3-basic luciferase vector (Promega, Madison, WI). A mutated reporter construct was generated by changing the HRE from ACGTGGG to AAAAGGG and made to mirror the p5xHRE generated by Shibata et al. (43). Reporter plasmids were cotransfected with a constitutively expressed Renilla luciferase plasmid (pHRL-TK; Promega) using the Lipofectamine Plus Reagent (Life Technologies). Luciferase activity was determined using the Dual Luciferase System (Promega) and normalized to Renilla luciferase activity.

### Western Blot

Cultured BM-MPCs were placed in hyperoxia or hypoxia for 24 h. Nuclear protein was obtained using Pierce Nuclear and Cytoplasmic Extraction Reagents (Pierce Biotechnology, Rockford, IL) according to the manufacturer's instructions. Protein content was standardized using the BCA Protein Assay kit (Pierce Biotechnology). Nuclear protein (20 μg) was separated by SDS-PAGE on 7.5% gels, transferred to polyvinylidene difluoride membranes, and blocked with 5% milk in tris-buffered saline with Tween. Protein detection was performed with primary antibodies for HIF-1α (Novus Biologicals, Littleton, CO), with β-actin serving as an internal loading control (Lab

Vision, Fremont, CA). Blots were subsequently incubated with a horseradish peroxidase–conjugated secondary antibody (Amersham Biosciences, Piscataway, NJ). Blots were developed with ECL reagent (Amersham Biosciences) and exposed for 1–10 min on Kodak Biomax-MS film. Band densities were quantified with ImageJ software (National Institutes of Health).

### VEGF ELISA and Quantitative RT-PCR

Conditioned medium was obtained from BM-MPCs cultured at various oxygen tensions. VEGF levels were assayed using a Quantikine murine VEGF ELISA kit (R&D Systems, Minneapolis, MN) in accordance with the manufacturer's protocol. Total RNA was isolated from STZ exposed and nonexposed WT BM-MPCs using an RNeasy Mini kit (Qiagen, Hilden, Germany) according to the manufacturer's instructions. Total RNA was eluted in RNAse-free water and quantified using a spectrophotometer at 260 and 280 nm. On the same day, first-strand cDNA was synthesized by reverse transcription of 50 ng total RNA using the SuperScript III First-Strand Synthesis System (Life Technologies) with random hexamers as primers. For PCR reactions, we used TaqMan Assays-on-Demand Gene Expression Products from Applied Biosystems (Foster City, CA): *Vegf-α*, assay identification no. Mm01281447_m1. Gene expression levels were normalized to *Gapdh* expression, assay no. Mm99999915_g1, and presented as relative values. PCR was repeated three times for each assay.

### Migration Assay

BM-MPCs ($2 \times 10^4$ cells) suspended in DMEM were seeded on the upper chamber of 8-μm pore-size Transwell plates (Corning Costar, Corning, NY). For the hypoxia group, BM-MPCs were incubated in 1% oxygen for 24 h prior to commencement of the assay. At time zero, 100 nmol/L recombinant murine CXCL12 (R&D Systems) was added to the bottom chamber. Plates were placed in 21% oxygen and the cells allowed to migrate for 6 h at 37°C. Nonmigrating cells were removed from the top surface of the upper chamber using a cotton tip applicator. Migrating cells adhering to the undersurface of the upper chamber were counted by DAPI (Freund-Vector, Marion, IA) positivity. A total of five random fields of each membrane were analyzed using a Zeiss Axioplan 2 microscope (×200 magnification).

### Proliferation Assay

BM-MPCs ($2 \times 10^3$) were seeded in 96-well plates and serum starved in DMEM containing 1% FBS for 24 h to induce quiescence. Medium was then changed to fully supplemented medium (10% FBS) and cultured at varying oxygen tensions. At 18 h, BrdU (Cell Proliferation ELISA, BrdU; Roche, Basel, Switzerland) was added to the medium, and after an additional 6 h, cell proliferation was assayed according to the manufacturer's instructions. For assessment of direct STZ effects on BM-MPCs, immediately after induction of quiescence, BrdU was added to STZ exposed and nonexposed WT BM-MPCs, and after an additional 6 h, cell proliferation was assayed according to the manufacturer's instructions.

### Matrigel Tubule Assay

Matrigel (BD Biosciences, San Diego, CA) was thawed and placed in four-well chamber slides at 37°C for 30 min to allow solidification. BM-MPCs ($1 \times 10^5$) were plated alone in Matrigel and incubated at 37°C under 21% or 1% oxygen for 18 h. BM-MPCs ($5 \times 10^4$) were also coplated with $5 \times 10^4$ PKH26-labeled murine bEND.3 endothelial cells (American Type Culture Collection, Manassas, VA) in Matrigel and incubated under the same conditions. Tubule formation was defined as a structure exhibiting a length four times its width. Tubule counts were determined in five random fields per well using an inverted Leica DMIL microscope at ×40 magnification.

### Glucose Uptake Assay

A glucose uptake colorimetric assay was performed on WT and type 1 diabetic BM-MPCs according to the manufacture's instructions (Sigma-Aldrich). Briefly, cultured BM-MPCs ($2 \times 10^3$) were seeded in 96-well plates and serum starved in DMEM containing 1% FBS for 24 h to induce quiescence (WT cells were cultured in normoglycemic medium, and type 1 diabetic cells were cultured in either normoglycemic or hyperglycemic medium). Cells were then glucose starved for 40 min in low-glucose buffer and stimulated with or without insulin for 20 min in the presence of 2-deoxyglucose. Cells were washed and lysed, and relative level of 2-deoxyglucose was determined via colorimetric readout.

### In Vivo Murine Ischemia Model

A reproducible model of graded soft tissue ischemia was created on the dorsum of mice as previously described (16). Briefly, a full-thickness (epidermis, dermis, and underlying adipose tissue) three-sided peninsular flap (1.25 × 2.5 cm) was created in the dorsal skin. The skin tissue was elevated from the underlying muscular bed, and a 0.13-mm-thick silicone sheet was inserted to separate the skin from the underlying tissue. The skin flap was sutured back into place with 6-0 nylon sutures. This model creates a systemic response to hypoxia through the production of a predictable gradient of HIF-1 and CXCL12 expression within the flap (16). The gradient of ischemia from proximal to distal was confirmed by tissue oximetry and color laser Doppler. Oxygen tensions were highest in the intact (cranial) portion of the raised peninsular tissue bed, and decreased in a graded fashion caudally along the flap (reaching a nadir of 2 mmHg in the most ischemic area of skin). Tissue oxygen levels recovered to their baseline values between 14 to 21 days after creation of the flap.

At designated time points (0, 0.5, 5, 7, 14, and 21 days), mouse bone marrow was harvested as described above. Mononuclear cells were also obtained by retro-orbital bleed followed by a red cell lysis (150 mmol/L $NH_4Cl$, 10 mmol/L $KHCO_3$, and 0.1 mmol/L EDTA for 5 min at 4°C). Blood and bone marrow were stained

with fluorescent antibodies against CD45 (PE; BD Biosciences), Sca-1 (FITC; eBiosciences, San Diego, CA), cKit (PE-Cy7; BD Biosciences), and lineage markers (Lin: TER119, B220, CD4, CD8, CD11b, and Gr-1 [PE-Cy5; eBiosciences]). Cells not stained with these antibodies were incubated with the appropriate isotype controls or left unstained. Cells were washed and analyzed using a FACSAria. Data were analyzed using FlowJo digital FACS software.

### Parabiosis Model and In Vivo Imaging

Parabiosis mice pairs were joined surgically using 4-0 silk sutures at the elbow and knee joints and 6-0 nylon suture along the skin edges of a full-thickness flank incision. Eight weeks after parabiosis, peninsular flaps were created on the backs of mice as described above but modified to include a single dorsal artery to prevent diabetic flap necrosis. Donor mice (right partner) expressed luciferase under the control of ActB (supplied by Dr. Christopher Contag, Stanford University). Recipient mice (left partner) were syngeneic on an FVB background (The Jackson Laboratory). Three months after ischemia, flaps were harvested and bathed in 150 mg/kg luciferin in PBS. Flaps were imaged using the IVIS Spectrum system (Caliper Life Sciences, Hopkinton, MA).

### Microfluidic Single-Cell Analysis

Fresh BM-MPCs with the surface marker profile $Lin^-/CD45^-/Sca\text{-}1^+$ were sorted as single cells into 10 μL lysis buffer using a BD FACSAria flow cytometer. With use of low-cycle preamplification, cDNA was obtained using Cells Direct (Life Technologies) with Taqman assay primer sets (Applied Biosystems) as per the manufacturers' specifications. cDNA was loaded onto the 48.48 Dynamic Array (Fluidigm, South San Francisco, CA) for quantitative PCR (qPCR) amplification using Universal PCR Master Mix (Applied Biosystems) with Taqman assay primer sets as previously described (44).

### Statistical Analysis

Results are presented as mean ± SEM. Data analysis was performed using either Student *t* test (migration and Matrigel assays) or one-way ANOVA (proliferation and VEGF ELISA). Results were considered significant for $P < 0.05$. Unless otherwise stated, all measurements were obtained from independent experiments performed at least in triplicate.

## RESULTS

We previously showed that diabetes attenuates local hypoxic upregulation of VEGF and other growth factors by decreasing transactivation by HIF-1α, leading to impaired angiogenesis (19). In this study, we sought to define whether diabetes also induces intrinsic functional impairments in recruited cells that may further contribute to observed deficits in ischemic neovascularization. We found that diabetic BM-MPCs have deficits in proliferation, migration, and tubulogenesis compared with WT cells.

Specifically, migration toward a CXCL12 stimulus, a peptide critical for progenitor cell chemotaxis in vasculogenesis (16), was blunted in diabetic BM-MPCs both in hyperoxia and in hypoxia (Fig. 1*A*). Genomic BrdU incorporation studies demonstrated that diabetic BM-MPCs proliferate less than WT BM-MPCs in hyperoxic and hypoxic conditions (Fig. 1*B*). Moreover, the ability of these diabetic BM-MPCs to form tubules in the presence of Matrigel was diminished in both hyperoxia and in hypoxia (Fig. 1*C*). None of these deficits were correctable by growing diabetic cells under normoglycemic culture conditions (1.0g/L glucose) (Fig. 1*A–C*).

In normal neovascularization, cells exposed to hypoxia stabilize the transcription factor HIF-1α, which drives expression of "vasculogenic" genes such as VEGF (45). We previously demonstrated HIF dysfunction in fibroblasts isolated from diabetic mice and traced this dysfunction to reactive oxygen species–induced methylglyoxal modification of HIF-1α rather than reduced HIF-1α protein levels (19).

Here, we examined HIF-1α activity in diabetic BM-MPCs subjected to hyperglycemic and hypoxic culture conditions. In contrast to what occurs in fibroblasts, diabetic BM-MPCs failed to significantly increase HIF activity in response to hypoxia (Fig. 1*D*), and Western blot analysis of diabetic BM-MPCs demonstrated lower levels of nuclear HIF-1α protein in both hyperoxia and hypoxia compared with BM-MPCs from WT mice (Fig. 1*E*). This resulted in deficits in VEGF protein production in response to hypoxia (Fig. 1*F*), consistent with previous observations in diabetic mice (46). Importantly, when these cells were transferred to normoglycemic culture conditions (1.0 g/L glucose) HIF stabilization and VEGF production were not normalized (Fig. 1*D–F*). Moreover, these persistent deficits were not explained by intracellular glucose availability alone, as glucose uptake was largely restored after culture of diabetic cells in normoglycemia (Supplementary Fig. 1). These findings demonstrate that diabetic BM-MPCs exhibit an impaired hypoxic response that results in attenuated vasculogenic protein production that is uncorrectable with glucose control.

To control for the possibility that the observed impairments in STZ-induced diabetic mice might be due to direct effects of the toxin on these cells, we evaluated the functional properties of WT cells treated with STZ in vitro (Supplementary Fig. 2). We found no significant differences in VEGF expression or proliferation in treated cells, suggesting that the observed impairments in cells harvested from diabetic mice are not due to direct effects of STZ on these cells.

Our in vitro data above suggest that dysfunction at the cellular level may compromise the mobilization and function of BM-MPCs in diabetes. To evaluate this, we compared the distributions of progenitor cells in the circulation of diabetic and WT mice at baseline and after a standardized ischemic insult.

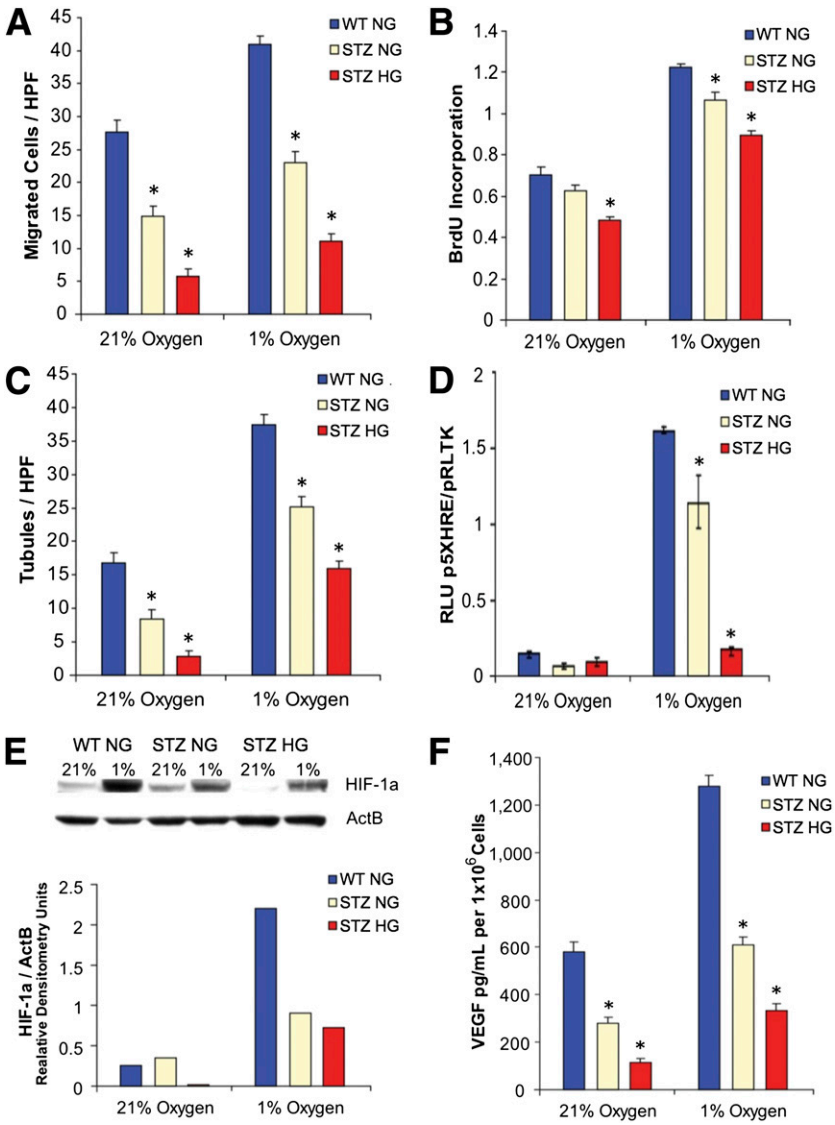


**Figure 1**—Diabetic BM-MPCs have poor baseline vasculogenic properties in hyperoxia and hypoxia, functions that cannot be corrected with return to normal glucose levels. MPCs isolated from the bone marrow of type 1 diabetic (modeled by STZ) and WT mice were cultured in either 21% oxygen (hyperoxia) or 1% oxygen (hypoxia) under either normoglycemic (NG) (1 g/L) or hyperglycemic (HG) (4.5 g/L) glucose conditions. Diabetic BM-MPCs under all culture conditions exhibited a diminished ability to migrate toward a CXCL12 stimulus, a peptide critical for progenitor cell chemotaxis in vasculogenesis (*A*); undergo proliferation based on genomic BrdU incorporation studies (*B*); and form tubules in Matrigel when cocultured with b.End3 cells (*C*). *D*: HIF-1α transcriptional activity in STZ diabetic BM-MPCs, as measured by a firefly luciferase reporter plasmid using the VEGF HRE. *E*: Immunoblot and densitometry for HIF-1α protein demonstrate that diabetic BM-MPCs fail to stabilize HIF-1α in hypoxia. *F*: Diabetic BM-MPCs produce less VEGF-A in hyperoxic and hypoxic conditions as measured by ELISA on conditioned medium. HPF, high power field; RLU, relative light units. *$P < 0.05$ vs. WT group, $n = 3$.

To define MPCs in the broadest possible way, we examined a primary bone marrow–derived population that is lineage negative, CD45 negative, and Sca-1 positive, which only excludes stem/progenitor cells of hematopoietic origin (11,17,47). To justify this exclusion, we demonstrate that only nonhematopoietic cells are mobilized from the bone marrow in response to ischemic injury (Supplementary Fig. 3).

Diabetic animals exhibited a dramatic decline in baseline levels of $Lin^-/CD45^-/Sca\text{-}1^+$ BM-MPCs in the bone marrow (Fig. 2*A*), as well as decreased mobilization of BM-MPCs to the peripheral circulation after ischemic insult (Fig. 2*B*). Again, this was not correctable after restoration of normal glucose levels for 6 months, demonstrating that these defects appear to be irreversible (Fig. 2*C*).

To further clarify the relative importance of previously described defects in hypoxic signaling (19,20,22,48) and intrinsic deficits in diabetic BM-MPCs, we used a murine model of parabiosis (Fig. 3*A*) (49). In this system, donor mice express luciferase under the control of ActB, which permits identification of cells that have trafficked across

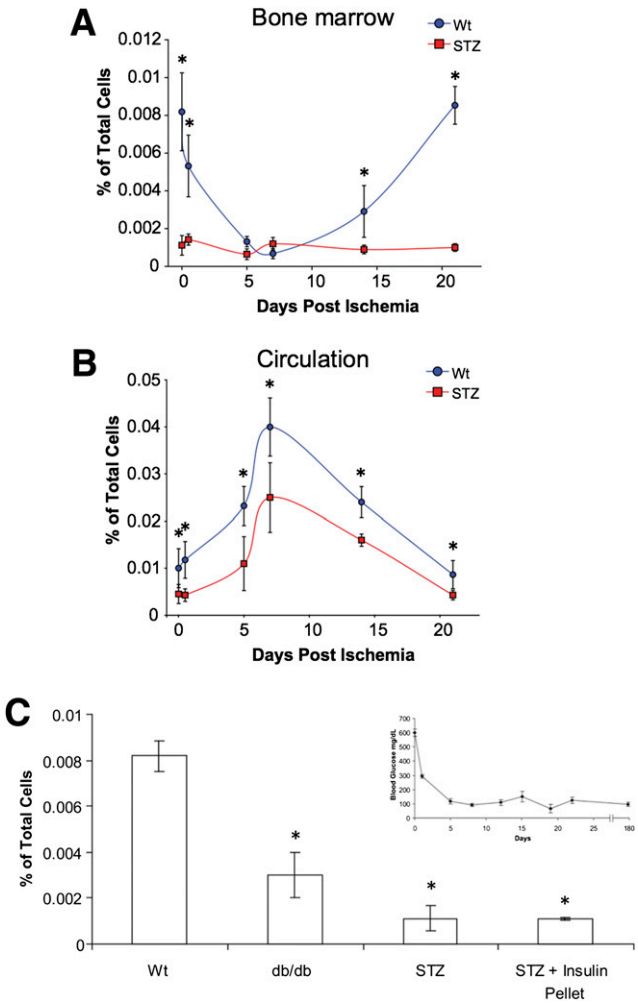


**Figure 2**—Diabetic and WT Lin$^-$/CD45$^-$/Sca-1$^+$ cells are mobilized from the bone marrow in response to peripheral ischemia. *A*: Bone marrow isolated from STZ-induced diabetic mice had significantly fewer Lin$^-$/CD45$^-$/Sca-1$^+$ cells compared with normal animals at baseline. *B*: Peripheral blood isolated from WT mice showed an increase in the number of circulating Lin$^-$/CD45$^-$/Sca-1$^+$ cells 7 days after surgery. Diabetic mice, in contrast, exhibited an attenuated response to peripheral ischemic insult. *C*: Baseline levels of Lin$^-$/CD45$^-$/Sca-1$^+$ cells from the bone marrow of normal, *db/db* mice, STZ diabetic mice, and STZ mice after 6 months of treatment with an insulin pellet. Hyperglycemic control failed to normalize levels of Lin$^-$/CD45$^-$/Sca-1$^+$ cells. *Inset*: STZ diabetic mice had insulin pellets implanted at day zero, and their glucose was monitored for 6 months, throughout which normoglycemic levels were maintained. *$P < 0.05$ vs. WT group.

the parabiotic interface to recipient ischemic tissue using optical imaging (Fig. 3*B*). Significant chimerism was evident in both normal and diabetic pairings at 10 days postparabiosis (data not shown). As previously reported (50), capillary blood glucose levels in mice with STZ-induced diabetes paired with nondiabetic mice did not normalize.

Ischemic tissue flaps were created on the dorsum of recipient mice, and this tissue was subsequently examined for the presence of donor BM-MPCs after 3 months in order to exclude the contribution of inflammation. Tissue isolated from WT←WT pairings demonstrated much higher levels of resident BM-MPCs than those from STZ←STZ pairings ($P < 0.05$) (Fig. 3*C* and *D*). Hybrid pairings (STZ←WT and WT←STZ) exhibited intermediate levels of cellular trafficking that were significantly different from STZ→STZ and WT←WT pairing ($P < 0.05$), but not from each other. (Mouse pairs are denoted according to recipient animal←donor animal.) Unpaired STZ mice also failed to increase SDF-1α expression after ischemic flap creation (Fig. 3*E*). These findings suggest that even with correction for peripheral signaling factors, intrinsic MPC defects limit the capacity of bone marrow–derived cells for ischemic trafficking in diabetic mice and may underlie impairments in soft tissue repair.

In the previous experiments, we demonstrated aggregate functional deficits in diabetic BM-MPCs and depletion of the bone marrow reservoir of these cells. However, since we have defined BM-MPCs using a very broad definition, these cells undoubtedly represent a markedly heterogeneous population (51,52), and it remained unclear whether these differences were due to a global dysfunction or selective depletion of a discrete functional subset. To differentiate these two possibilities, we interrogated cells at the single-cell level in order to elucidate differences that cannot be distinguished by traditional population-based analysis. Here, we used a previously described microfluidics-based single-cell gene expression analysis to identify transcriptional variation among diabetic BM-MPCs (44). Again, to cast the widest net, we isolated primary Lin$^-$/CD45$^-$/Sca-1$^+$ cells from the bone marrow of WT and diabetic mice and analyzed the simultaneous expression of >40 gene targets known to be highly relevant to vasculogenesis for each individual cell from each group (Supplementary Table 1). In order to control for any model-specific effects in the STZ mice, we also evaluated cells from leptin receptor–deficient (*db/db*) mice as a model of type 2 diabetes.

As expected, BM-MPCs exhibited significant transcriptional heterogeneity across all gene targets (Supplementary Figs. 4 and 5), and considerable variability in gene expression was observed across cells from both WT and diabetic mice (Fig. 4*A*). Single-gene analysis using Kolmogorov-Smirnov statistics identified eight genes with distributions of expression that were different between WT cells and those from type 1 or type 2 diabetic models ($P < 0.01$ after Bonferroni correction for multiple comparisons) (Fig. 4*B*), including the cell adhesion molecule *Vcam1* and chemokine *Cxcl12* (*Sdf1*), both thought to play key roles in ischemic neovascularization (16).

To determine whether this differential expression was attributable to a specific subset of WT or diabetic cells, we applied partitional clustering using a cluster estimation heuristic as previously described (53) (Supplementary Fig. 6). Three distinct, transcriptionally defined subpopulations of WT cells were identified (Fig. 4*C*). When these partitions were applied to diabetic cells, significantly

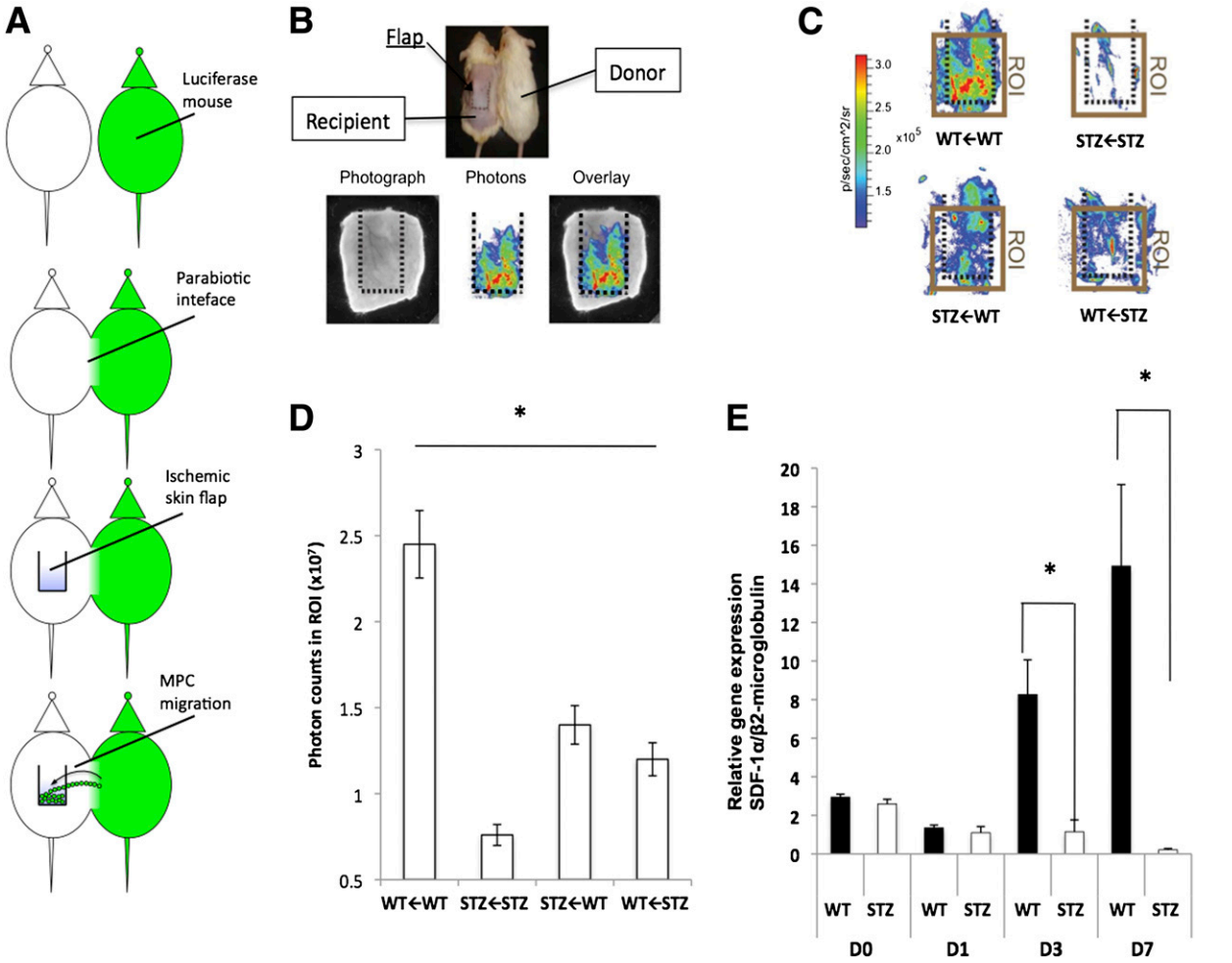


**Figure 3**—Diabetic BM-MPCs exhibit impaired cell trafficking in vivo; this cannot be corrected with restoration of WT signaling. *A*: Parabiosis schema. Luciferase-positive and control mice are joined surgically, creating a parabiotic interface. An ischemic skin flap is created on the dorsum of the control mouse, and the number of migrating (luciferase$^+$) cells was recorded using IVIS. *B*: Eight weeks after parabiosis, a modified ischemic flap is created on the back of the recipient mouse (*top*). Three months after ischemia, the ischemic flap from the recipient mouse is assayed for bioluminescence ex vivo (*bottom panel*). *C*: Heat maps of bioluminescence ex vivo imaging from WT←WT, STZ←STZ, STZ←WT, and WT←STZ pairings. Mouse pairs are denoted according to recipient animal←donor animal. *D*: Quantification of region of interest (ROI) from the ischemic flap area of each pairing. *E*: Transcriptional analysis of SDF-1α in ischemic flaps of WT and STZ mice at days 0, 1, 3, and 7 after flap creation. D, day; p, photons; sr, squared radian. *$P < 0.05$ vs. QT group.

fewer cells were found in the first two clusters (Fig. 4*D–F*). Notably, these clusters defined two subpopulations characterized by either elevated expression of vasculogenesis-related genes, such as *Cxcl12*, *Cdh2, Vcam1*, and *Anxa5* (cluster 1) (54), or elevated expression of genes associated with angiogenesis, including the endothelial cell receptor *Tek* (also known as *Tie2*) in association with the stem cell surface marker *Eng* (*Cd105*) (cluster 2). This suggests that these depleted populations may be progenitor cells further primed for endothelial cell differentiation (55).

## DISCUSSION

In this study, we delineate multiple deficits in diabetic BM-MPCs in vitro and in vivo that lead to impaired vasculogenic function and demonstrate that these deficits exist in tissues and circulating cells of diabetic animals. We attempted to reverse these effects by normalizing glucose levels and found that BM-MPCs displayed "diabetic memory," which suggests that diabetes causes permanent modifications in these cells that are passed to daughter cells with each division. As BM-MPC cultures have substantial heterogeneity, characterizing these changes is difficult using traditional molecular interrogation of entire populations of cells. Single-cell analysis avoids these confounding factors by defining each cell's transcriptome, which allows for greater understanding of the heterogeneous groups within diabetic and WT BM-MPCs. In this study, we elucidate transcriptional differences in diabetic cells on the single-cell level that offer insight into the dysfunction of diabetic BM-MPCs.

In a previous report, we identified a population of cells in vivo that were not HSCs and that responded to

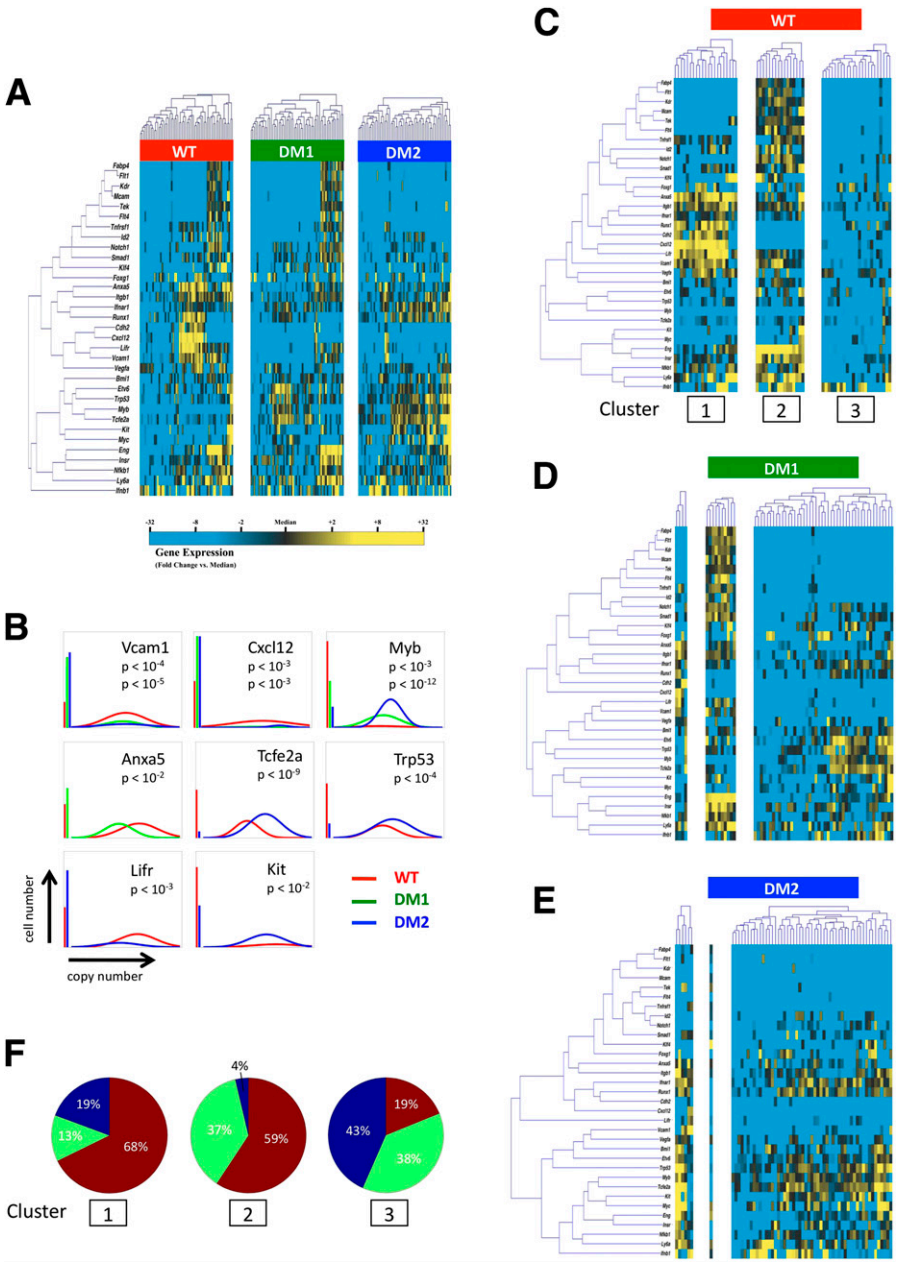


**Figure 4**—Single-cell qPCR of Lin$^-$/CD45$^-$/Sca-1$^+$ BM-MPCs. *A*: Hierarchical clustering of simultaneous gene expression for 60 individual cells from WT, STZ diabetic (DM1), and *db*/*db* (DM2) mice. Gene expression is presented as fold change from median on a color scale from yellow (high expression, 32-fold above median) to blue (low expression, 32-fold below median). See Supplementary Figs. 4 and 5 for complete data set. *B*: Differentially expressed genes between WT and diabetic (STZ [DM1] or *db*/*db* [DM2]) cells identified using non-parametric two-sample Kolmogorov-Smirnov testing. Eight genes exhibit significantly different ($P < 0.01$ after Bonferroni correction for multiple comparisons) distributions of single-cell expression between populations, illustrated here using median-centered Gaussian curve fits. The left bar for each panel represents the fraction of qPCR reactions that failed to amplify in each group. Curves and *P* values for each gene are shown only for those diabetic groups significantly different from WT cells. *C*: *K*-means clustering of WT cells, with $k = 3$ chosen using the gap statistic as described in Supplementary Fig. 6. *D* and *E*: Cells from STZ-induced (DM1) and *db*/*db* (DM2) animals were partitioned into subgroups according to the cluster centroids of the WT cells in *C*. *F*: Pie graphs representing the fraction of cells comprising each cluster from WT (red), STZ diabetic (green), and *db*/*db* (blue) animals.

ischemic injury (17). Here, we show that diabetes impairs the proangiogenic function of this population—a pattern not seen in HSCs. In addition, we demonstrate that diabetes induces lasting epigenetic changes in BM-MPCs, which causes dysfunction after correction of hyperglycemia. Specifically, we correlate transcriptional dysfunction with the functional deficits seen in diabetes. In vivo, we scrutinized these cells individually and demonstrated significantly fewer diabetic cells that express a highly vasculogenic transcriptional signature. Single-cell transcriptional analysis of

primary $Lin^-/CD45^-/Sca\text{-}1^+$ cells showed that these cells are heterogeneous even when they are tightly sorted by FACS as a small fraction of the total plated BM-MPC population. Moreover, we have identified a subset of cells in the WT $Lin^-/CD45^-/Sca\text{-}1^+$ population that are highly provascular and less prevalent in diabetic BM-MPC populations. This suggests that diabetic mice are fundamentally deficient in bone marrow–derived vascular progenitor cells, and this deficiency may also explain the observed decreased levels of EPCs from diabetic patients in clinical trials (22).

Since these subpopulations appear to be more pluripotent and provascular, it is possible that deficits in these specific populations may underlie the aggregate functional deficits observed in diabetes, suggesting that isolation and purification of these cells could be expected to improve the effectiveness of BM-MPCs for use in regenerative medicine and bioengineering applications. Furthermore, our in vitro and in vivo data demonstrate that these defects are irreversible. This suggests that cell-based therapeutics using autologous cells may be unlikely to succeed in correcting the effects of prolonged glucose exposure and impact the phenomenon of metabolic memory. While additional studies of these distinct subpopulations of BM-MPCs will be required to prove the functional differences suggested by their gene expression, these data suggest that autologous stem cell–based therapies in diabetic patients may be limited by intrinsic deficits in important progenitor cell populations and that new strategies focusing on healthy (nondiabetic) progenitor cells may be required.

**Duality of Interest.** No potential conflicts of interest relevant to this article were reported.

**Author Contributions.** M.J. designed the study, performed the experiments, developed the mathematical framework, and wrote the manuscript. M.S. designed the study, performed the experiments, developed the mathematical framework, and wrote the manuscript. J.P.G. designed the study, performed the experiments, and wrote the manuscript. I.N.V. designed the study and performed the experiments. Z.N.M., R.C.R., D.D., and H.T. performed the experiments. M.T.L. provided intellectual input and aided in experimental design. A.J.B. developed the mathematical framework, provided intellectual input, and aided in experimental design. G.C.G. designed the study and wrote the manuscript. G.C.G. is the guarantor of this work and, as such, had full access to all the data in the study and takes responsibility for the integrity of the data and the accuracy of the data analysis.

## References

1. Zimmet P, Alberti KG, Shaw J. Global and societal implications of the diabetes epidemic. Nature 2001;414:782–787

2. Annual number (in thousands) of new cases of diagnosed diabetes among adults aged 18–79 years, United States, 1980–2010 [article online], 2010. Available from http://www.cdc.gov/diabetes/statistics/incidence/fig1.htm. Accessed 14 June 2013

3. Narayan KM, Boyle JP, Geiss LS, Saaddine JB, Thompson TJ. Impact of recent increase in incidence on future diabetes burden: U.S., 2005-2050. Diabetes Care 2006;29:2114–2116

4. Caro JJ, Ward AJ, O'Brien JA. Lifetime costs of complications resulting from type 2 diabetes in the U.S. Diabetes Care 2002;25:476–481

5. Fox CS, Coady S, Sorlie PD, et al. Increasing cardiovascular disease burden due to diabetes mellitus: the Framingham Heart Study. Circulation 2007;115:1544–1550

6. Moss SE, Klein R, Klein BE. Cause-specific mortality in a population-based study of diabetes. Am J Public Health 1991;81:1158–1162

7. Glotzbach JP, Wong VW, Gurtner GC. Neovascularization in diabetes. Expert Rev Endocrinology 2010;5:99–111

8. Abaci A, Oğuzhan A, Kahraman S, et al. Effect of diabetes mellitus on formation of coronary collateral vessels. Circulation 1999;99:2239–2242

9. Jude EB, Oyibo SO, Chalmers N, Boulton AJ. Peripheral arterial disease in diabetic and nondiabetic patients: a comparison of severity and outcome. Diabetes Care 2001;24:1433–1437

10. Takahashi T, Kalka C, Masuda H, et al. Ischemia- and cytokine-induced mobilization of bone marrow-derived endothelial progenitor cells for neovascularization. Nat Med 1999;5:434–438

11. Tepper OM, Capla JM, Galiano RD, et al. Adult vasculogenesis occurs through in situ recruitment, proliferation, and tubulization of circulating bone marrow-derived cells. Blood 2005;105:1068–1077

12. Ceradini DJ, Gurtner GC. Homing to hypoxia: HIF-1 as a mediator of progenitor cell recruitment to injured tissue. Trends Cardiovasc Med 2005;15:57–63

13. Rafii S, Lyden D. Therapeutic stem and progenitor cell transplantation for organ vascularization and regeneration. Nat Med 2003;9:702–712

14. Semenza GL, Agani F, Booth G, et al. Structural and functional analysis of hypoxia-inducible factor 1. Kidney Int 1997;51:553–555

15. Ben-Shoshan J, Schwartz S, Luboshits G, et al. Constitutive expression of HIF-1alpha and HIF-2alpha in bone marrow stromal cells differentially promotes their proangiogenic properties. Stem Cells 2008;26:2634–2643

16. Ceradini DJ, Kulkarni AR, Callaghan MJ, et al. Progenitor cell trafficking is regulated by hypoxic gradients through HIF-1 induction of SDF-1. Nat Med 2004;10:858–864

17. Hamou C, Callaghan MJ, Thangarajah H, et al. Mesenchymal stem cells can participate in ischemic neovascularization. Plast Reconstr Surg 2009;123(Suppl.):45S–55S

18. Velazquez OC. Angiogenesis and vasculogenesis: inducing the growth of new blood vessels and wound healing by stimulation of bone marrow-derived progenitor cell mobilization and homing. J Vasc Surg 2007;45(Suppl A):A39–A47

19. Thangarajah H, Yao D, Chang EI, et al. The molecular basis for impaired hypoxia-induced VEGF expression in diabetic tissues. Proc Natl Acad Sci U S A 2009;106:13505–13510

20. Lerman OZ, Galiano RD, Armour M, Levine JP, Gurtner GC. Cellular dysfunction in the diabetic fibroblast: impairment in migration, vascular endothelial growth factor production, and response to hypoxia. Am J Pathol 2003;162:303–312

21. El-Ftesi S, Chang EI, Longaker MT, Gurtner GC. Aging and diabetes impair the neovascular potential of adipose-derived stromal cells. Plast Reconstr Surg 2009;123:475–485

22. Tepper OM, Galiano RD, Capla JM, et al. Human endothelial progenitor cells from type II diabetics exhibit impaired proliferation, adhesion, and incorporation into vascular structures. Circulation 2002;106:2781–2786

23. Ceradini DJ, Yao D, Grogan RH, et al. Decreasing intracellular superoxide corrects defective ischemia-induced new vessel formation in diabetic mice. J Biol Chem 2008;283:10930–10938

24. Baksh D, Song L, Tuan RS. Adult mesenchymal stem cells: characterization, differentiation, and application in cell and gene therapy. J Cell Mol Med 2004;8:301–316

25. Crosby JR, Kaminski WE, Schatteman G, et al. Endothelial cells of hematopoietic origin make a significant contribution to adult blood vessel formation. Circ Res 2000;87:728–730

26. Kondo M, Wagers AJ, Manz MG, et al. Biology of hematopoietic stem cells and progenitors: implications for clinical application. Annu Rev Immunol 2003;21:759–806

27. Massengale M, Wagers AJ, Vogel H, Weissman IL. Hematopoietic cells maintain hematopoietic fates upon entering the brain. J Exp Med 2005;201:1579–1589

28. Balsam LB, Wagers AJ, Christensen JL, Kofidis T, Weissman IL, Robbins RC. Haematopoietic stem cells adopt mature haematopoietic fates in ischaemic myocardium. Nature 2004;428:668–673
29. Wagers AJ, Sherwood RI, Christensen JL, Weissman IL. Little evidence for developmental plasticity of adult hematopoietic stem cells. Science 2002;297: 2256–2259
30. Udani VM, Santarelli JG, Yung YC, et al. Hematopoietic stem cells give rise to perivascular endothelial-like cells during brain tumor angiogenesis. Stem Cells Dev 2005;14:478–486
31. Oswald J, Boxberger S, Jørgensen B, et al. Mesenchymal stem cells can be differentiated into endothelial cells in vitro. Stem Cells 2004;22:377–384
32. Reyes M, Dudek A, Jahagirdar B, Koodie L, Marker PH, Verfaillie CM. Origin of endothelial progenitors in human postnatal bone marrow. J Clin Invest 2002; 109:337–346
33. Wang X, Hisha H, Taketani S, et al. Characterization of mesenchymal stem cells isolated from mouse fetal bone marrow. Stem Cells 2006;24:482–493
34. Psaltis PJ, Zannettino AC, Worthley SG, Gronthos S. Concise review: mesenchymal stromal cells: potential for cardiovascular repair. Stem Cells 2008; 26:2201–2210
35. Silva GV, Litovsky S, Assad JA, et al. Mesenchymal stem cells differentiate into an endothelial phenotype, enhance vascular density, and improve heart function in a canine chronic ischemia model. Circulation 2005;111:150–156
36. Yue WM, Liu W, Bi YW, et al. Mesenchymal stem cells differentiate into an endothelial phenotype, reduce neointimal formation, and enhance endothelial function in a rat vein grafting model. Stem Cells Dev 2008;17:785–793
37. Caplan AI. Why are MSCs therapeutic? New data: new insight. J Pathol 2009;217:318–324
38. Crisan M, Yap S, Casteilla L, et al. A perivascular origin for mesenchymal stem cells in multiple human organs. Cell Stem Cell 2008;3:301–313
39. Kucia MJ, Wysoczynski M, Wu W, Zuba-Surma EK, Ratajczak J, Ratajczak MZ. Evidence that very small embryonic-like stem cells are mobilized into peripheral blood. Stem Cells 2008;26:2083–2092
40. Charbord P. Bone marrow mesenchymal stem cells: historical overview and concepts. Hum Gene Ther 2010;21:1045–1056
41. McEvoy RC, Andersson J, Sandler S, Hellerström C. Multiple low-dose streptozotocin-induced diabetes in the mouse. Evidence for stimulation of a cytotoxic cellular immune response against an insulin-producing beta cell line. J Clin Invest 1984;74:715–722
42. Strandell E, Sandler S. In vitro response to interleukin-1 beta and streptozotocin in pancreatic islets isolated from male and female nonobese diabetic mice. J Endocrinol 1997;153:81–86
43. Shibata T, Giaccia AJ, Brown JM. Development of a hypoxia-responsive vector for tumor-specific gene therapy. Gene Ther 2000;7:493–498
44. Glotzbach JP, Januszyk M, Vial IN, et al. An information theoretic, microfluidic-based single cell analysis permits identification of subpopulations among putatively homogeneous stem cells. PLoS ONE 2011;6:e21211
45. Semenza GL. Surviving ischemia: adaptive responses mediated by hypoxia-inducible factor 1. J Clin Invest 2000;106:809–812
46. Ceradini DJ, Yao D, Grogan RH, et al. Decreasing intracellular superoxide corrects defective ischemia-induced new vessel formation in diabetic mice. J Biol Chem 2008;283:10930–10938
47. Thangarajah H, Vial IN, Chang E, et al. IFATS collection: Adipose stromal cells adopt a proangiogenic phenotype under the influence of hypoxia. Stem Cells 2009;27:266–274
48. Kang L, Chen Q, Wang L, et al. Decreased mobilization of endothelial progenitor cells contributes to impaired neovascularization in diabetes. Clin Exp Pharmacol Physiol 2009;36:e47–e56
49. Kamran P, Sereti KI, Zhao P, Ali SR, Weissman IL, Ardehali R. Parabiosis in mice: a detailed protocol. J Vis Exp 2013;80:e50556
50. Pietramaggiori G, Scherer SS, Alperovich M, Chen B, Orgill DP, Wagers AJ. Improved cutaneous healing in diabetic mice exposed to healthy peripheral circulation. J Invest Dermatol 2009;129:2265–2274
51. da Silva Meirelles L, Caplan AI, Nardi NB. In search of the in vivo identity of mesenchymal stem cells. Stem Cells 2008;26:2287–2299
52. Phinney DG, Hill K, Michelson C, et al. Biological activities encoded by the murine mesenchymal stem cell transcriptome provide a basis for their developmental potential and broad therapeutic efficacy. Stem Cells 2006;24:186–198
53. Tibshirani R, Walther G, Hastie T. Estimating the number of clusters in a dataset via the gap statistic. J R Statistic Soc B 2001;63:441–423
54. Peichev M, Naiyer AJ, Pereira D, et al. Expression of VEGFR-2 and AC133 by circulating human CD34(+) cells identifies a population of functional endothelial precursors. Blood 2000;95:952–958
55. Asahara T, Masuda H, Takahashi T, et al. Bone marrow origin of endothelial progenitor cells responsible for postnatal vasculogenesis in physiological and pathological neovascularization. Circ Res 1999;85:221–228